is folded through the upper half-plane back along the negative real axis as shown in Figure 7-6, the cuts representing the singularities of $\mathbf{G}(p')$. Since D^u is analytic in the upper half-plane, it has no discontinuity across the left G-cut. By using the relation

$$\mathbf{G}(\mathbf{p}, p_0 + i\,\delta) = \mathbf{G}^*(\mathbf{p}, p_0 - i\,\delta) \tag{7-65}$$

that is, the values of $\mathbf{G}$ on opposite sides of the cut are related by complex conjugation (see Section 5-4), the deformed contour can be replaced by an integral along the lower side of the cut if $\mathbf{G}(p)$ is replaced by $\mathbf{G}(p) - \mathbf{G}^*(p) = 2i\,\mathrm{Im}\,\mathbf{G}(p)$. Therefore the D^u-piece of Σ^{ph} is given by

$$\begin{aligned}\boldsymbol{\Sigma}_u^{\mathrm{ph}}(p) = \frac{-2m}{(2\pi)^3|\mathbf{p}|}\int_{-\infty}^{0} dp_0' \\ \times \mathrm{Im}\left\{\int_{-\infty}^{\infty} d\epsilon' \frac{[Z'p_0'\mathbf{1} - \phi'\tau_1]}{(Z'p_0')^2 - \phi'^2 - \epsilon'^2 + i\,\delta}\right\} \\ \times \sum_\lambda \int_0^{2k_F} q\,dq\{\tilde{g}_{q\lambda}\}^2 D_\lambda^u(q, p_0 - p_0')\end{aligned} \tag{7-66}$$

On performing the ϵ'-integral one obtains the expression

$$\begin{aligned}\boldsymbol{\Sigma}_u^{\mathrm{ph}}(p) = \frac{m}{(2\pi)^2|\mathbf{p}|}\int_{-\infty}^{0} dp_0'\,\mathrm{Re}\left\{\frac{Z'p_0'\mathbf{1} - \phi'\tau_1}{[(Z'p_0')^2 - \phi'^2]^{1/2}}\right\} \\ \times \sum_\lambda \int_0^{2k_F} q\,dq\{\tilde{g}_{q\lambda}\}^2 D_\lambda^u(q, p_0 - p_0')\end{aligned} \tag{7-67}$$

In a similar manner the term coming from D^l can be handled by folding into the lower half-plane the portion of the p_0'-contour originally along the negative real axis, as shown in Figure 7-7.

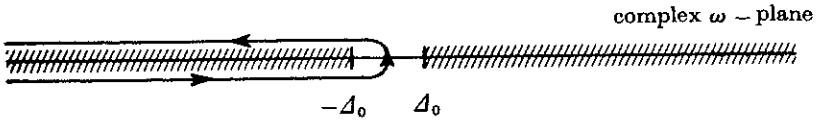

FIGURE 7-6 Folded contour for evaluating Σ_u^{ph}.

velocity-depende e
correct form in s
we mentioned ab... o
order $(m/M)^{1/2} \simeq 10^{-2}$.

We now turn to the problem of reducing the Coulomb term in the equation for Σ, (7-61), to one-dimensional form.[123] Unfortunately, the potential $\mathscr{V}_c(p - p')$ does not decrease rapidly for $|p_0 - p_0'| > \omega_D$, as is the case for the phonon interaction. For this reason the p_0'-integral is not limited to the region $|p_0'| < \omega_c$, as it was above, and the trick of integrating first with respect to the three-momentum does not work here in a straightforward way. To get around this complication we would like to introduce a pseudo-potential which accounts for the Coulomb interaction in (7-61) outside of the energy interval $-\omega_c < p_0' < \omega_c$. This general approach was first discussed by Bogoliubov, Tolmachev, and Shirkov[52] and reformulated by Morel and Anderson[124] to treat pairing correlations in He^3. To determine the pseudo-potential we consider the Coulomb part of the electron self-energy

$$\mathbf{\Sigma}^c(p) = i \int \tau_3 \mathbf{G}(p') \tau_3 \mathscr{V}_c(p - p') \frac{d^4p'}{(2\pi)^4} \tag{7-71}$$

If we define ϕ^c, χ^c, and $(1 - Z)^c p_0$ to be the coefficients of τ_1, τ_3, and $\mathbf{1}$, respectively, in $\mathbf{\Sigma}^c$ we have

$$\phi^c(p) = -i \int \frac{d^4p'}{(2\pi)^4} \frac{\phi'}{(Z'p_0')^2 - \bar{\epsilon}'^2 - \phi'^2} \mathscr{V}_c(p - p') \tag{7-72a}$$

$$\chi^c(p) = i \int \frac{d^4p'}{(2\pi)^4} \frac{\bar{\epsilon}'}{(Z'p_0')^2 - \bar{\epsilon}'^2 - \phi'^2} \mathscr{V}_c(p - p') \tag{7-72b}$$

$$[1 - Z(p)]^c p_0 = i \int \frac{d^4p'}{(2\pi)^4} \frac{Z'p_0'}{(Z'p_0')^2 - \bar{\epsilon}'^2 - \phi'^2} \mathscr{V}_c(p - p') \tag{7-72c}$$

For simplicity we assume that $\mathscr{V}_c(p - p')$ is well represented by a statically screened potential so that it is independent of p_0 and p_0'. Since the left-hand side of (7-72c) is antisymmetric in p_0 and the right-hand side is independent of p_0, we find $[1 - Z(p)]^c = 0$. We also neglect χ^c since its main effect is to

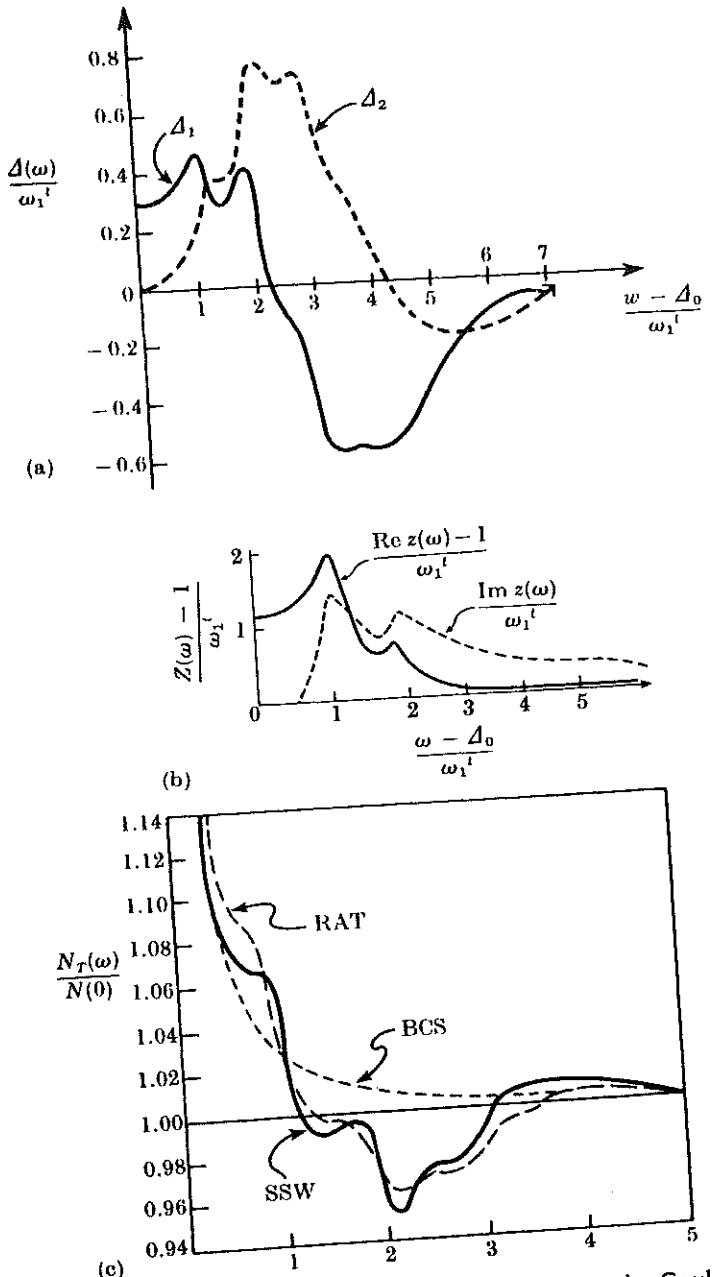

FIGURE 7-9 (a) The same as Figure 7-8 except the Coulomb pseudopotential is set equal to a value roughly appropriate for lead, $N(0)U_c = 0.11$. (b) The real and imaginary parts of the renormalization function $Z(\omega)$ for this case. (c) Tunneling density of states.

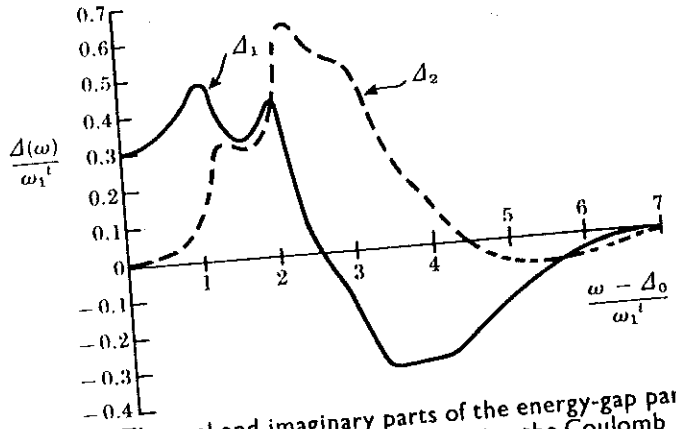

FIGURE 7-8 The real and imaginary parts of the energy-gap parameter Δ plotted as a function of energy for lead, setting the Coulomb pseudopotential equal to zero.

producing a sharp drop in N_T. A similar situation obtains near the longitudinal phonon emission threshold. Thus a peak in the phonon density of states is reflected by a knee or peak in N_T followed by a rapid drop in this function. A good deal of detailed information about the phonon density of states can be gained in this manner from the I–V tunneling curves. In particular, van Hove singularities in the phonon spectrum along with more general singularities are reflected in d^2I/dV^2. These have been discussed by Scalapino and Anderson.[127]

It is interesting to note that the electron–phonon coupling is so strong for lead that the quasi-particle picture is meaningless over much of the energy spectrum. Nevertheless, the Green's function approach is sufficiently powerful and simple to allow this problem to be treated in detail. Furthermore, one finds structure in measurable quantities, e.g., $N_T(E)$, over energy intervals which are small compared to the level width one would calculate in perturbation theory. This is due to the fact that the spectral weight function $A(\mathbf{p}, \omega)$ is distinctly non-Lorentzian in form in this case.

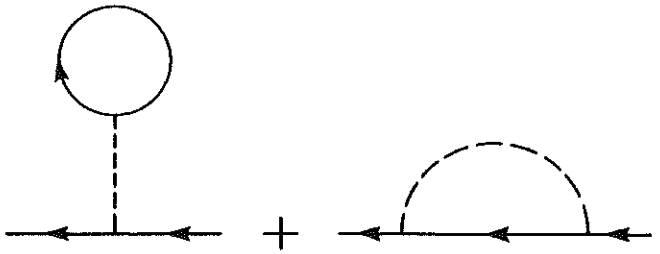

FIGURE 7-5 Contributions to Σ within the Hartree–Fock approximation. The electron lines include the self-consistently determined self-energy Σ.

If the poles of $G_0(\mathbf{p}, p_0)$ are to be unaffected by Σ, we must require the self-consistency condition

$$\Sigma(\mathbf{p}, \bar{\epsilon}_p) = 0 \tag{7-24}$$

to be satisfied. Since in our particular problem Σ is independent of p_0, we have the familiar Hartree–Fock relation

$$\chi_p = \int_{\bar{\epsilon}_{p'}<0} \frac{d^3p'}{(2\pi)^3} \{2\langle \mathbf{p}, \mathbf{p}'|V|\mathbf{p}, \mathbf{p}'\rangle - \langle \mathbf{p}', \mathbf{p}|V|\mathbf{p}, \mathbf{p}'\rangle\} \tag{7-25}$$

determining χ_p.

While this appears to be a complicated way of phrasing the HF approximation, the scheme is easily extended to include the pairing correlations. The idea is simply to generalize the linearization (7-10) to include Hartree-like terms involving $\langle 0|c_1{}^+c_2{}^+|0\rangle$ and $\langle 0|c_3c_4|0\rangle$. The state $|0\rangle$ is then to be determined self-consistently as in the standard Hartree–Fock approach.

At this point one might argue that since the full Hamiltonian commutes with the total number of particles operator N_{op}, the exact eigenstates of H are eigenfunctions of N_{op}. One might then argue that our approximate state $|0\rangle$ should also be chosen to be an eigenfunction of N_{op} and therefore the Hartree-like terms $\langle 0|c_1{}^+c_2{}^+|0\rangle$ and $\langle 0|c_3c_4|0\rangle$ vanish identically. We can make two counter arguments. First, in the limit of a large system the ground states of the N_0 and the $N_0 + \nu$ particle system are degenerate for $|\nu| \ll N_0$, if the origin of energy is shifted by

For simplicity we consider the case of zero center-of-mass momentum for the interacting pair of electrons (i.e., a $\mathbf{q} = 0$ pair, as in the Cooper problem). We then seek the values of q_0 such that (7-5) is satisfied. By inserting the expression for G_0 and carrying out the k_0-integral by residues, one readily finds that (7-5) reduces to

$$\frac{1}{\lambda_0} = \sum_{|\mathbf{k}|>k_F} \frac{|w_k|^2}{q_0 - 2\epsilon_k} - \sum_{|\mathbf{k}|<k_F} \frac{|w_k|^2}{q_0 - 2\epsilon_k} \equiv \tilde{\Phi}(q_0) \qquad (7\text{-}6)$$

where we have replaced $\int d^3k/(2\pi)^3$ by $\sum_k$ since we are interested in drawing an analogy with the solutions of the Cooper problem (2-11) for $\mathbf{q} = 0$. If $|w_k|^2$ were zero for states below the Fermi surface, (2-11) and (7-6) would be identical. By allowing the interaction to extend down into the Fermi sea, the states below the Fermi surface play a role in determining the singularities of t. A plot of the right-hand side of (7-6) is shown in Figure 7-4. For $\lambda_0 > 0$ (i.e., a repulsive potential) the perturbed states are again trapped between the unperturbed levels and no bound states

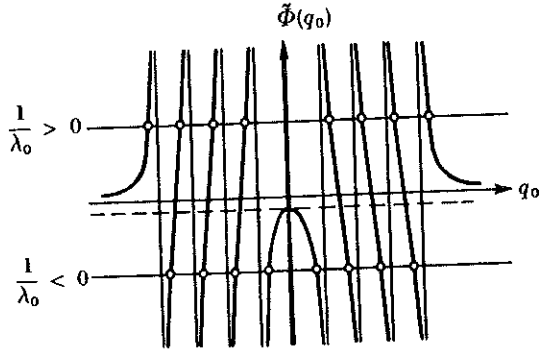

FIGURE 7-4 A plot of the function $\tilde{\Phi}(q_0)$ which determines the poles of the t-matrix in the many-body system. For a repulsive s-wave interaction ($\lambda_0 > 0$), all poles are real. For an attractive interaction ($\lambda_0 < 0$), two pure imaginary poles of t appear (regardless of the strength $|\lambda_0|$ if one considers the limit of a large system). These poles illustrate the instability of the normal phase at $T = 0$ for an attractive two-body interaction.

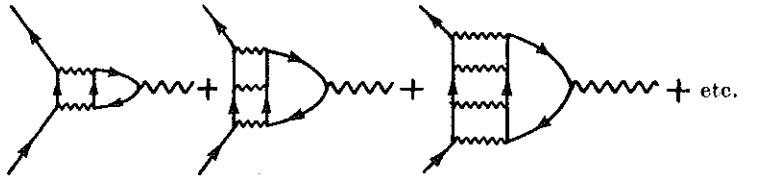

FIGURE 7-3 A class of ladder graphs which contributes to the electron–phonon vertex function Γ and leads to the superconductor instability.

One can readily establish this relation by performing an iteration solution of (7-1) in powers of $\mathscr{V}$ and noticing that one generates the desired series. While this integral equation cannot be solved in general, a solution is immediate if we replace $\mathscr{V}(q)$ by a non-retarded factorizable s-wave potential which is finite in a shell around the Fermi surface

$$\mathscr{V}(p - k) = \lambda_0 w_{\mathbf{p}}^* w_{\mathbf{k}} \tag{7-2}$$

where

$$w_{\mathbf{k}} = \begin{cases} 1 & |\epsilon_k| < \omega_c \\ 0 & \text{otherwise} \end{cases}$$

Then one finds the solution

$$\langle k' + q, -k'|t|k + q, -k\rangle = \frac{\lambda_0 w_{\mathbf{k}'+\mathbf{q}}^* w_{\mathbf{k}+\mathbf{q}}}{1 - i\lambda_0 \int |w_{\mathbf{p}+\mathbf{q}}|^2 G_0(p + q) G_0(-p) \dfrac{d^4p}{(2\pi)^4}} \tag{7-3}$$

which can be checked by direct substitution.

If we are able to show that t is ill-behaved, then Γ will also be ill-behaved since in our approximation Γ is given by

$$\Gamma(p, q) = g_q\left[1 - i \int \langle p, k + q|t|p + q, k\rangle G_0(k) G_0(k + q) \frac{d^4k}{(2\pi)^4}\right] \tag{7-4}$$

(see Figure 7-3). From (7-3) we see that t will be singular when the denominator vanishes, that is, when

$$\frac{1}{\lambda_0} = i \int |w_{\mathbf{p}+\mathbf{q}}|^2 G_0(k + q) G_0(-k) \frac{d^4k}{(2\pi)^4} \tag{7-5}$$

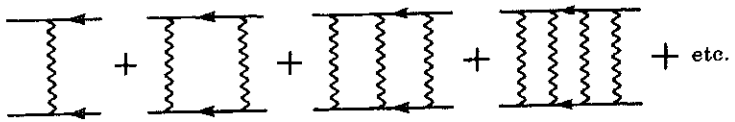

FIGURE 7-1 The ladder-graph series.

scatter each other corresponding to the two-particle problem discussed by Cooper.[41] It is clear that the series of ladder graphs shown in Figure 7-1 represents such an effect. If the effective potential is attractive, one would expect to find a bound state of the two-particle system, or an instability of the system as a whole. To understand how these graphs would enter $\Sigma(p)$, one need only close one of the electron lines onto itself as shown in Figure 7-2. If we reinterpret the graphs of this figure in terms of G, D, and Γ it follows that the instability is due to the singular behavior of Γ resulting from the graphs shown in Figure 7-3 [see (6-38)].

In order to understand the instability in more detail we consider the ladder graph series of Figure 7-1. Except for the external electron lines, the sum of the series is given by the "t"-matrix, defined by

$$\begin{aligned}\langle k' + q, -k'|t|k + q, -k\rangle &= \mathscr{V}(k' - k) \\ &+ i\int \mathscr{V}(k' - k'')G_0(k'' + q)G_0(-k'') \\ &\times \langle k'' + q, -k''|t|k + q, -k\rangle \frac{d^4k''}{(2\pi)^4} \qquad (7\text{-}1)\end{aligned}$$

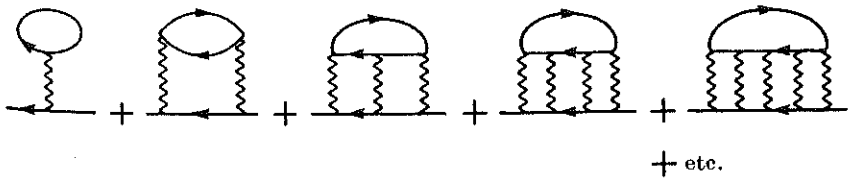

FIGURE 7-2 The ladder approximation for Σ.